CONF-891093--5

BNL-43284

Characterization of Rh Films on Ta(110)

BNL--43284

DE90 001323

L. Q. Jiang, M. W. Ruckman, and Myron Strongin
Physics Department
Brookhaven National Laboratory
Upton, NY 11973-6000

PACS: 68.55-a, 73.60.Aq, 82.65My

DISCLAIMER

The submitted manuscript has been authored under contract DE-AC02-76CH00016 with the Division of Materials Sciences, U. S. Department of Energy. Accordingly, the U. S. Government retains a non-exclusive, royalty-free license to publish or reproduce the published form of this contribution, or allow others to do so, for U. S. Government purposes.

Characterization of Rh Films on Ta(110)

L. Q. Jiang, M. W. Ruckman, and Myron Strongin
Physics Department
Brookhaven National Laboratory
Upton, NY 11973-6000

Abstract

The surface and electronic structure of Rh films on Ta(110) up to several monolayers thick on Ta(110) are characterized by photoemission, Auger emission, low energy electron diffraction and low energy ion scattering. From the variation of the Rh Auger peak-to-peak intensity as a function of evaporation time, Rh/Ta(110) appears to grow in the Stranski-Krastanov mode at room temperature. However, the LEIS data shows that the Rh adatoms begin to cluster on Ta(110) before growth of the monolayer is completed. Diffuse LEED scattering suggests that the Rh films are disordered. Photoemission shows that Rh chemisorption on Ta(110) generates two peaks located at 1.2 and 2.5 eV binding energy during the initial phase of thin film growth ($0 < \theta <$ 0.5 ML). By 0.75 ML Rh coverage, those states merge into a broad structure centered near 2 eV binding energy. Photoemission peaks typical of a Rh(111) surface are seen at higher coverages ($\theta > 3.7$ ML). Photoemission data for CO covered surfaces shows that CO dissociates on the Rh/Ta(110) surface for Rh coverages less than 2.5 ML and also shows that the Rh clusters develop at least one site capable of molecular CO adsorption above 0.3 ML Rh coverage.

Introduction

Rhodium is an important industrial catalyst and also used in automotive catalytic converters to reduce nitrogen oxides.[1] Surface techniques are used in a number of studies which examine the interaction of small molecules and hydrocarbons with single crystal Rh surfaces.[2-8] More recent studies have examined the catalytic properties of Rh clusters and small particles,[9] Rh/Al_2O_3[10,11], TiOx/Rh,[12,13] and Ag/Rh(111).[14] It is well known that transition metal monolayers on transition metal substrates have altered surface, electronic, and chemical properties.[15-20] Tauster and Fung[21] first suggested that bonding between the substrate and thin metal films or particles is responsible for the change in catalytic properties. Ruckman et al.[15,16] used photoemission data to show that CO has a negligible sticking coefficient on Pd monolayers on Ta(110) at 300K, and that the CO-Pd bond is weaker for the Pd monolayer when compared to thicker Pd(111) layers. This work also suggested that changes in the density of states near the Fermi level are responsible for this behavior. Recently, Koel and coworkers[17] published temperature programmed desorption (TPD) measurements showing an 18.6 Kca/mole reduction in the activation energy for CO desorption from Pd/Ta(110) monolayers when compared to Pd(111).[22] The properties of thin Rh films on transition metal substrates are not as thoroughly studied as those of Pd films and such information would be of value in understanding the physics and chemistry of Rh catalysts.

In this paper we report results for a study of the growth and electronic structure of thin Rh films on Ta(110) and their interaction with CO. Low energy ion scattering (LEIS) and low energy electron diffraction (LEED) show that Rh forms three dimensional islands at 300K. Photoemission shows that

Rh-Ta bonding takes place and also shows that CO both dissociates and molecularly adsorbs on ultrathin Rh overlayers.

Experimental Procedure

Surface studies of Rh/Ta(110) were conducted in an ultra high vacuum system equipped for LEED, AES, LEIS, and ultra-violet photoemission spectroscopy. Synchrotron radiation-based photoemission studies were conducted in another UHV system installed on the U7B beamline at the Brookhaven National Synchrotron Light Source (NSLS). Photoemission, AES, and LEIS were conducted using a double-pass CMA. Our LEIS experimental set-up is similar to that described by Vurens et al.[23] A sputter ion gun (Perkin-Elmer model 04-300) operated at 500 eV in a 2×10^{-6} Torr helium atmosphere produced the He^+ beam for LEIS. For photoemission, the pass energy was set to 25 eV and the sample was oriented with the sample normal ~42° from the CMA axis and ~45° from the incident photon beam.

The substrate is a Ta(110) crystal grown by high temperature recrystallization of a Ta foil (for details see reference 24). The crystal was large enough to show the sharp hexagon-like LEED pattern expected for a Ta(110) surface. Surface cleaning was done by resistive heating cycles (~2500K for 1-5 sec) and our surface experiments show only negligible levels of contamination.

Rhodium was deposited using a resistively heated coiled Rh filament and the current was kept constant at 7A during deposition cycles. It was found, this procedure gives reproducible depositions of monolayer amounts of Rh in two minute intervals. An evaporation rate monitor was used to monitor the amount of Rh deposited but our surface studies do not indicate that Rh grows

layer-by-layer on Ta(110). Hence, the expression of Rh coverages (θ) monolayer units (1 ML Rh = 1.6 x 10^{15} Rh atoms/cm^2) is intended to provide information about the amount of Rh deposited and not the thickness of the Rh overlayer. CO dosing was conducted at a CO partial pressure of 5 x 10^{-8} Torr in a turbo-pumped chamber. The ion pump was valved off to minimize CO gas contamination and gas purity was checked using a quadrupole mass spectrometer.

Results and Discussion

A. Growth and Structure of Rh Films on Ta(110)

The dependence of the Rh $M_{4,5}VV$ (302 eV) and Ta $N_{4,5}VV$ (179 eV) Auger peaks as a function of evaporation time (AST curve) is shown in figure 1. The growth of the Rh peak and the attenuation of the Ta peak is linear up to two minutes. At about two minutes, the slope of each curve changes and the curves are non-linear for longer evaporations. The AST plot indicates that a break occurs in the gradient at two minutes elapsed time and this usually indicates that a monolayer has formed.[25] The observation of no further breaks is consistent with the layer-plus-islanding (Stranski Krastanov (SK)) growth mechanism.[26]

Rh(111) has a slightly larger in-plane density of atoms than Pd(111) and both Rh(111) and Pd(111) monolayers have significantly larger in-plane atomic densities than the Ta(110) surface. Pd/Ta(110) was found to grow epitaxially on Ta(110) and has a (1x1) LEED pattern at submonolayer coverage.[24] At monolayer coverage, a complex LEED pattern similar to that found for Pd/Nb (110) by Sagurton et al.[27] is seen. Sagurton et al. suggested this (1x7) LEED pattern is due to multiple scattering of LEED beams from a Pd(111)-like

overlayer by the Ta(110) substrate. Multilayer Pd coverages show a LEED pattern like Pd(111).[28,29] LEED studies of Rh covered Ta(110) found that Rh deposition caused a significant increase in diffuse LEED scattering and weakened the sharp spots due to the Ta(110) substrate. At higher Rh coverages, faint and fuzzy LEED spots due to Rh(111) were seen along with a considerable amount of diffuse scattering. The diffuse scattering suggests disorder or surface roughness[32] and the faint Rh(111) spots are probably due to the formation of small Rh(111) crystallites.

LEIS was done on Rh/Ta(110) to check the conclusion derived from the AST plot concerning the SK growth mechanism. Figure 2(a) shows a LEIS spectrum obtained for a two minute Rh deposition, i.e., AST break point and "monolayer" Rh coverage. 500 He^+ ions are scattered from this surface at two distinct energies and a hard sphere scattering calculation shows that the component at 0.86 is due to Rh and the other component at 0.92 is due to Ta. In figure 2(b), the normalized intensity of the Ta peak is plotted as a function of evaporation time. This curve suggests that the deposition of more than 2 ML (4 minutes) of Rh is needed to completely cover the surface and also shows that clustering plays a major role in the growth of the Rh overlayer. Extrapolation of the attenuation rate of the Ta peak for short evaporation times suggests that the growth of two dimensional Rh islands would lead to complete coverage of Ta by two minutes evaporation time. The failure to completely cover the surface at 2 minutes evaporation time indicates that the clustering begins at submonolayer coverage. We conclude that Rh film growth on Ta(110) is an example of the Volmer-Weber (3d islanding) growth mechanism[26] rather than the SK growth mechanism.

B. Photoemission Studies of Rh/Ta(110)

Photoemission showed that interaction between Pd monolayers and Nb or Ta substrates greatly modifies the electronic structure. Band structure and density of states calculations[30] for Pd/Nb(110) show that considerable hybridization of the Pd 5sp-4d and Nb 5s-4d states takes place at the interface and that the density of states near the Fermi energy E_f is greatly reduced on the surface atom layer. This has a significant affect on surface reactivity with simple molecules like CO. (Note: Hoffman points out in a recent review article[32] that the states near E_F are derived from the frontier orbitals which play a crucial role in chemical bond formation with adsorbates.) The chemical interaction between Pd and Nb causes the Pd d-band to shift away from E_f and become narrower. Good agreement between theory and experiment was found by El-Batannouy et al.[30] and Williams et al.[31] for Pd/Nb(110) and the strong correlation between spectra for Pd/Ta(110) and Pd/Nb(110) suggested to Ruckman et al.[24] that the bonding between Pd and Ta was similar. Other investigators find similar changes in the overlayer electronic states for Pd/W(110),[19] Pt/W(110),[33] and the affect of interfacial bonding on electronic structure is seen for other bimetallic systems - most notably Cu/Ru(0001).[20]

Figure 3 shows photoemission spectra (He I (21.2 eV)) for a range of Rh coverages on Ta(110). Spectra for a monolayer Rh coverage and a thick ($\theta > 5$ ML) Rh film as a function of photon energy are shown in figures 4(a) and (b). Interpretation of the photoemission spectra is more difficult for Rh/Ta(110) than for Pd/Ta(110) because the islanding produces a wider range of Rh adatom environments. At low coverages ($0 < \theta < 0.47$ ML), the islands are small or the Rh sits on the surface as adatoms. Rh adsorption produces a single peak

near -2.5 eV binding energy. A second peak near -1.5 eV becomes visible between 0.38 and 0.47 ML Rh coverage. The Ta valence band states near Ef decrease in intensity and change in shape with increasing Rh coverage. The modification of the Ta valence band states and the shift of the Rh derived-states to higher binding energy when compared to the thick Rh film (figure 4(b)) suggest that hybridization of the Rh 5s-4d and Ta 6s-5d bands occurs. Deposition of more Rh ($\Theta > 0.47$) produces a clustered or disordered Rh overlayer. At monolayer Rh coverage (figure 3), new states near 2 eV become the strongest states and there is a significant increase in the density of states just below E_f. For multilayer coverages (θ = 3.75 ML), the valence band broadens and begins to resemble that calculated for Rh.[34]

Synchrotron radiation photoemission[31] showed that certain parts of the Pd/Nb(110) valence band had emission from Nb and Pd components leading to their identification as interface related states. Houston et al. published similar findings for Cu/Ru(0001)[20] and Ni/Ru(0001)[35] based on angle-resolved photoemission. Both Rh and Ta show significant changes in photoemission cross section in the photon range 40 to 80 eV. The Rh valence states go through a minimum (48 eV) above the 4p threshold (37 eV) and are resonantly enhanced by the 4p-4d interaction between 55 and 75 eV.[36] The Ta valence states are most intense between 50 and 60 eV and decrease faster in intensity than those of Rh.[37] Figure 4(a) shows photoemission from a monolayer coverage of Rh as a function of photon energy. The peak near E_f (identified with the Ta substrate) and the peak near -2.8 eV binding energy are most intense between 46 and 55 eV photon energy. The peak near -1.3 eV is the largest feature above 55 eV photon energy. According to Williams et al.,[31] a correlation can be drawn between the cross section dependence of the metals and their contribution hybridized bonding and anti-bonding states. The state

near -2.8 eV has Ta-5d as well as Rh 4d contributions because it is resonantly enhanced near the Ta-5p threshold. The state near -1.3 eV shows its relationship with the Rh 4d states rather than the Ta 5d states because it is not resonantly enhanced near the Ta-5p threshold. We believe the state near -2.8 eV is an interface bonding state because it has both Rh-4d and Ta-5d components.

C. Carbon Monoxide Adsorption on Rh/Ta(110)

Figure 5 shows photoemission spectra for a 20 L (1L = 10^{-6} Torr-sec) CO exposure of Rh/Ta(110) surfaces at 300K. Vertical lines going from higher to lower binding energy mark the CO 4σ, 1π-5δ, and O 2p peaks, respectively. CO dissociates on Ta(110) and the molecular CO peaks are absent. On Rh(111), CO adsorbs molecularly with an activation energy for desorption of 31.6 Kcal/mole in the limit of zero coverage.[2] The activation energy decreases with CO coverage and at 300K a 1/4 ML of CO is retained on the surface. Castner et al.[2] reported that CO dissociates on stepped Rh surfaces and argue that CO should dissociate on rough Rh surfaces. Yates et al.[38] presented data which argues that the dissociation of CO on stepped or rough surfaces is unlikely. For our thickest Rh overlayer (θ = 10 ML), we find only the molecular CO photoemission features and see no evidence of CO dissociation.

We concluded from LEIS that Rh clusters and the surface layer has both Ta and Rh atoms. Photoemission from molecular and dissociated CO is observed for thin ($0.3 < \theta < 2.5$ ML) Rh films. Since CO normally dissociates on Ta(110) at 300K, we cannot determine whether CO also dissociates at the edges or the surfaces of the Rh islands. The intensity of the O 2p feature decreases with increasing Rh coverage. At 2.5 ML Rh coverage, where the

surface is almost fully covered by Rh, the molecular CO peaks are the largest CO related feature but they are much weaker than those for the thick Rh film. Similar behavior is seen for Pd/Ta(110)[15,16] and it was argued that the strength of the CO peaks is proportional to the amount of CO present on the surface. A TPD experiment like that done by Koel's group for Pd/Ta(110) is needed to determine whether the changes in photoemission from CO are directly connected to changes in CO coverage and to determine whether the strength of the CO-Rh bond changes as a function of thin film coverage.

Summary and Conclusions

Using several different techniques to investigate the structure of Rh films on Ta(110), we find that Rh forms 3d islands on Ta(110) at low coverage (θ < 5 ML), and that the surface has both Ta and Rh adsorption sites. Considerable diffuse LEED scattering from this surface prevents detailed structural studies and suggests the surface is highly disordered or rough. Photoemission suggests that the Rh 5s-4d and Ta 6s-5d bands hybridize and this has the greatest affect on photoemission from submonolayer Rh overlayers. We identify a Rh induced state near -2.5 eV binding energy as a possible Rh-Ta bonding state. CO dissociates as well as molecularly adsorbs on thin Ta(110)-supported Rh films. Additional research is being conducted to study the affect of the substrate on the chemical behavior of thin Rh films. Similar work is underway on Rh/Mo(110) which grows layer-by-layer and TPD will be used to accurately determine CO coverages and the activation energy for CO desorption.

Acknowledgment

The authors thank F. Loeb and his staff for technical assistance. Part of this work was done at the National Synchrotron Light Source which is supported by the United States Department of Energy. This research is supported by the U. S. DOE, Division of Materials Science, Contract No. DE-AC02-76CH00016.

References

1. K. C. Taylor in Catalysis and Automotive Pollution Control, Vol. 30 of Studies in Surface Science and Catalysis, A. Crucq and A. Rennel eds., Elsevier, Amsterdam, 1987 p 97.
2. D. G. Castner, B. A. Sexton, and G. A. Somorjai, Surf. Sci. 71, 519 (1978).
3. R. J. Koestner, M. A. van Hove, and G. A. Somorjai, Surf. Sci., 107,439 (1981).
4. V. V. Gorodetskii and B. E. Nieuwenhuys, Surf. Sci., 105, 299 (1981).
5. E. G. Seebauer, A. C. F. Kong, and L. D. Schmidt, Appl. Surf. Sci., 31, 163 (1988).
6. P. A. Thiel, E. D. Williams, J. T. Yates Jr., and W. H. Weinberg, Surf. Sci., 84, 54 (1979).
7. G. A. Del Angel, B. Coq, G. Ferrat, and F. Figueras, Surf. Sci., 156, 943 (1985).
8. L. A. De Louise and N. Winograd, Surf. Sci. 138, 417 (1984); L. A. De Louise, L. J. White, and N. Winograd, Surf. Sci. 147, 252 (1984).
9. Y. Zhu and L. D. Schmidt, Surf. Sci. 129, 107 (1983).
10. D. N. Belton and J. J. Schmeig, Surf. Sci. 202, 238 (1988).
11. R. C. Jaklevic, L. Elie, and H. C. Yao, Surf. Sci. 171, 279 (1988).
12. M. E. Levin, M. Salmeron, A. T. Bell, and G. A. Somorjai, Surf. Sci. 195, 429 (1988).
13. K. J. Williams, M. Salmeron, A. T. Bell, and G. A. Somorjai, Surf. Sci. 204, L745 (1988).
14. H. C. Peebles, D. D. Beck, J. M. White, and C. T. Cambell, Surf. Sci., 150, 120 (1985).

15. M. W. Ruckman and Myron Strongin, Phys. Rev. B 29, 7105 (1984).

16. M. W. Ruckman, P. D. Johnson, and Myron Strongin, Phys. Rev. B 31, 3405 (1985).

17. D. L. Neiman and B. E. Koel in Physical and Chemical Properties of Thin Metal Overlayers and Alloy Surfaces, D. M. Zehner and D. W. Goodman eds., (Materials Research Society, Pittsburgh, PA, 1987 p 143).

18. Shen Xinyin, D. J. Frankel, J. C. Hermanson, G. J. Lapeyre, and R. J. Smith, Phys. Rev. B 32, 2120 (1985).

19. G. W. Graham, J. Vac. Sci. Technol., A4, 760 (1986).

20. J. E. Houston, C. H. F. Peden, P. J. Feibelman, and D. R. Hamann, Phys. Rev. Lett., 56, 375 (1986); J. E. Houston, C. H. F. Peden, D. S. Blair, and D. W. Goodman, Surf. Sci. 167, 427 (1986).

21. S. J. Tauster and S. C. Fung, J. Catalysis, 55, 29 (1978).

22. H. Conrad, G. Ertl, J. Koch, and E. E. Latta, Surf. Sci. 43, 462 (1974).

23. G. Vurens, M. Salmeron, and G. A. Somorjai, Surf. Sci. 201, 129 (1988).

24. M. W. Ruckman, V. Murgai, and Myron Strongin, Phys. Rev. B 34, 1920 (1986).

25. D. P. Woodruff and T. A. Delchar, Modern Techniques of Surface Science, (Cambridge Univ. Press, Cambridge UK 1986, p 144).

26. J. A. Venables and G. D. T. Spiller in Surface Mobilities on Solid Surfaces, V. T. Bink ed., (Plenum, NY, 1981 p. 339); K. Reichelt, Vacuum 38, 1083 (1988).

27. M. Sagurton, Myron Strongin, F. Jona, and J. Colbert, Phys. Rev. B 27, 4580 (1983).

28. L. J. Clarke, Surface Crystallography - An Introduction to Low Energy Electron Diffraction, (Wiley, NY 1985) p. 218.

29. G. C. Wang, T.-M. Lu, and M. G. Lagally, J. Chem. Phys. 69, 479 (1978).

30. M. El-Batanouny, D. R. Hamann, S. R. Chubb, and J. W. Davenport, Phys. Rev. B 27, 2527 (1983); V. Kumar and K.-H. Bennemann, Phys. Rev. B 28, 3138 (1983).

31. G. P. Williams, M. El-Batanouny, J. Colbert, E. Jensen, and T. N. Rhodin, Phys. Rev. B 25, 3658 (1982).

32. R. Hoffman, Rev. Mod. Phys. 60, 601 (1988).

33. R. A. Demmin, R. L. Kurtz, R. L. Stockbauer, D. R. Mueller, and A. Shih (preprint).

34. V. L. Moruzzi, J. F. Janak, and A. R. Williams, Calculated Electronic Properties of Metals (Pergamon, NY, 1978) p. 140; D. A. Papaconstantopoulos, Handbook of the Bank Structure of Elemental Solids, (Plenum, NY 1986) p. 153.

35. J. E. Houston, J. M. White, P. J. Feibelman, and D. R. Hamann, Phys. Rev. B 38, 12164 (1988).

36. H. Hochst and M. K. Kelly, Phys. Rev. B 30, 1708 (1984).

37. J. J. Yeh and I. Lindau, Atomic and Nuclear Data Tables, 32, 1 (1985).

38. J. T. Yates Jr., E. D. Williams, and W. H. Weinberg, Surf. Sci. 91, 562 (1981); J. T. Yates Jr., E. D. Williams, and W. H. Weinberg, Surf. Sci. 115, L93 (1982).

Figure Captions

1. Auger peak amplitude versus evaporation time curves for the Rh M4,5VV and Ta N4,5VV transitions. A break in the slope is marked by a vertical dashed line.
2. (a) LEIS spectrum for a monolayer Rh film on Ta(110).
   (b) Normalized intensity (I/I_o) for the 0.92 Ta LEIS peak as a function of Rh coverage.
3. Photoemission spectra (h = 21.2 eV) for various Rh coverages on Ta(110).
4. (a) Photoelectron EDCs for a Rh monolayer on Ta(110) over photon energies from 40 to 80 eV.
   (b) Photoemission spectra for a thick Rh film for 40 $<h\nu<$ 80 eV.
5. Photoemission ($h\nu$ = 70 eV) for 20 L CO exposures of selected Rh/Ta(110) surfaces.

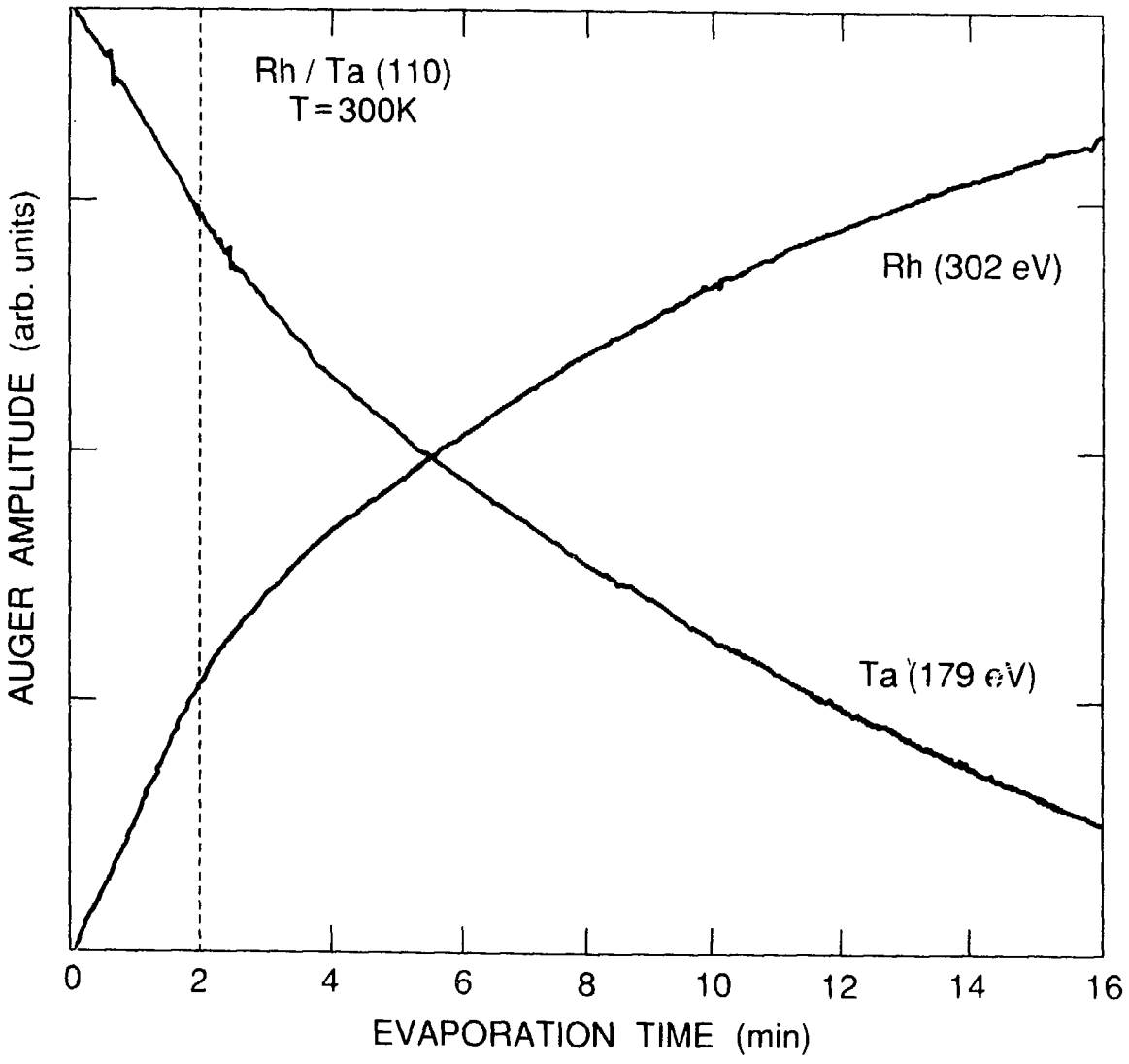
Rh / Ta (110)
T = 300K
Rh (302 eV)
Ta (179 eV)
AUGER AMPLITUDE (arb. units)
0
2
4
6
8
10
12
14
16
EVAPORATION TIME (min)

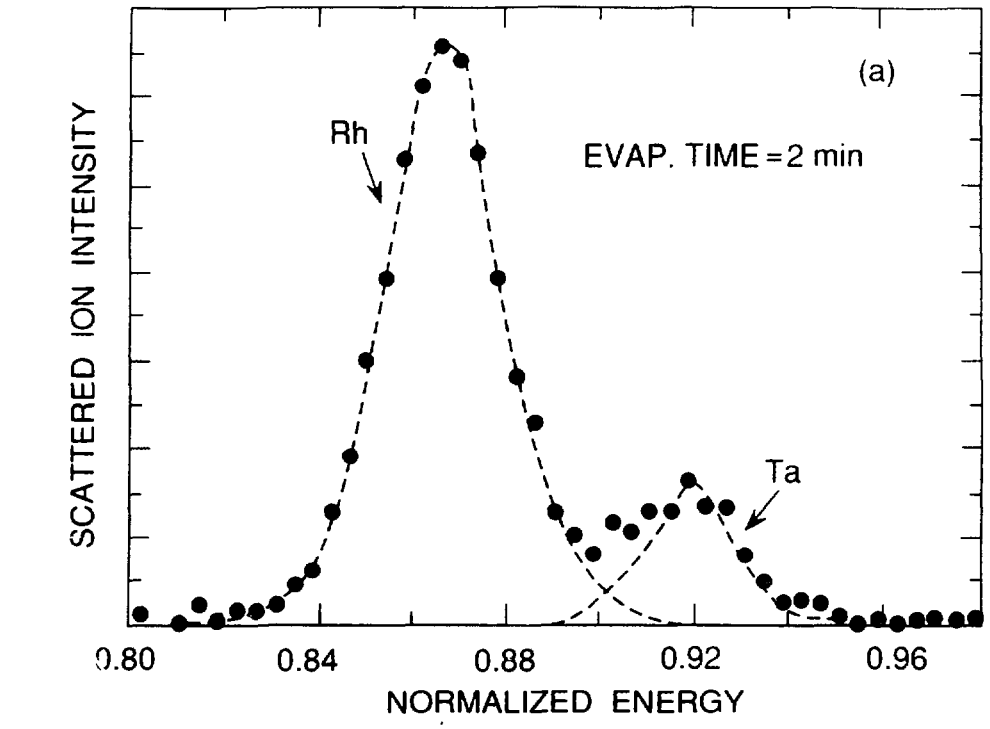
(a)
Rh
EVAP. TIME = 2 min
Ta
SCATTERED ION INTENSITY
0.80
0.84
0.88
0.92
0.96
NORMALIZED ENERGY

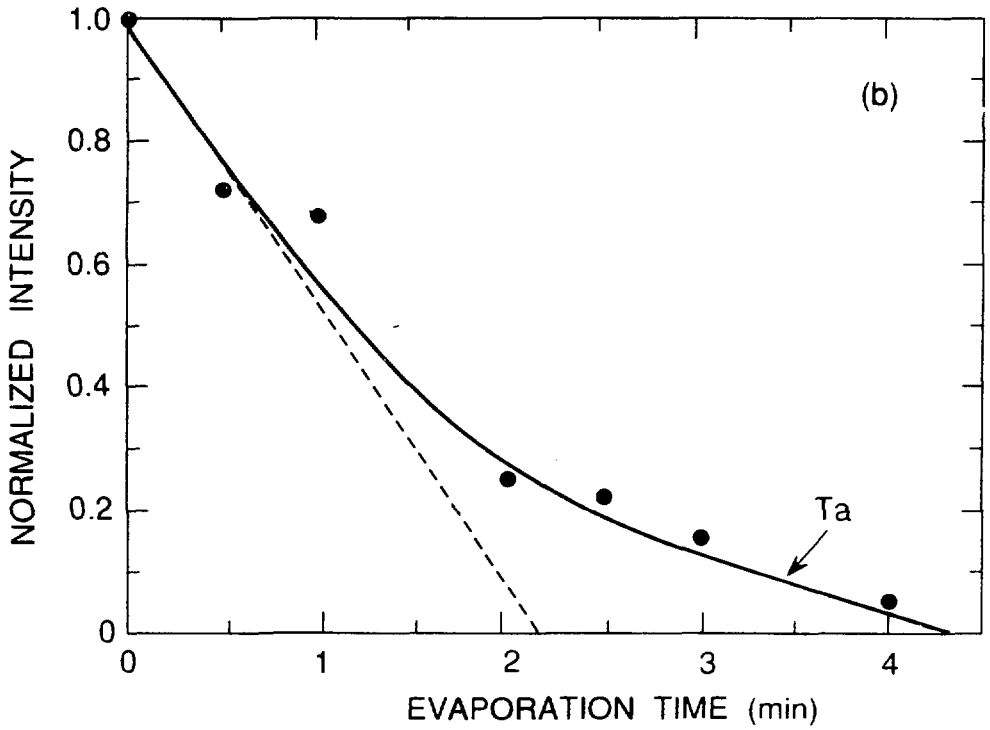
(b)
Ta
NORMALIZED INTENSITY
1.0
0.8
0.6
0.4
0.2
0
0
1
2
3
4
EVAPORATION TIME (min)

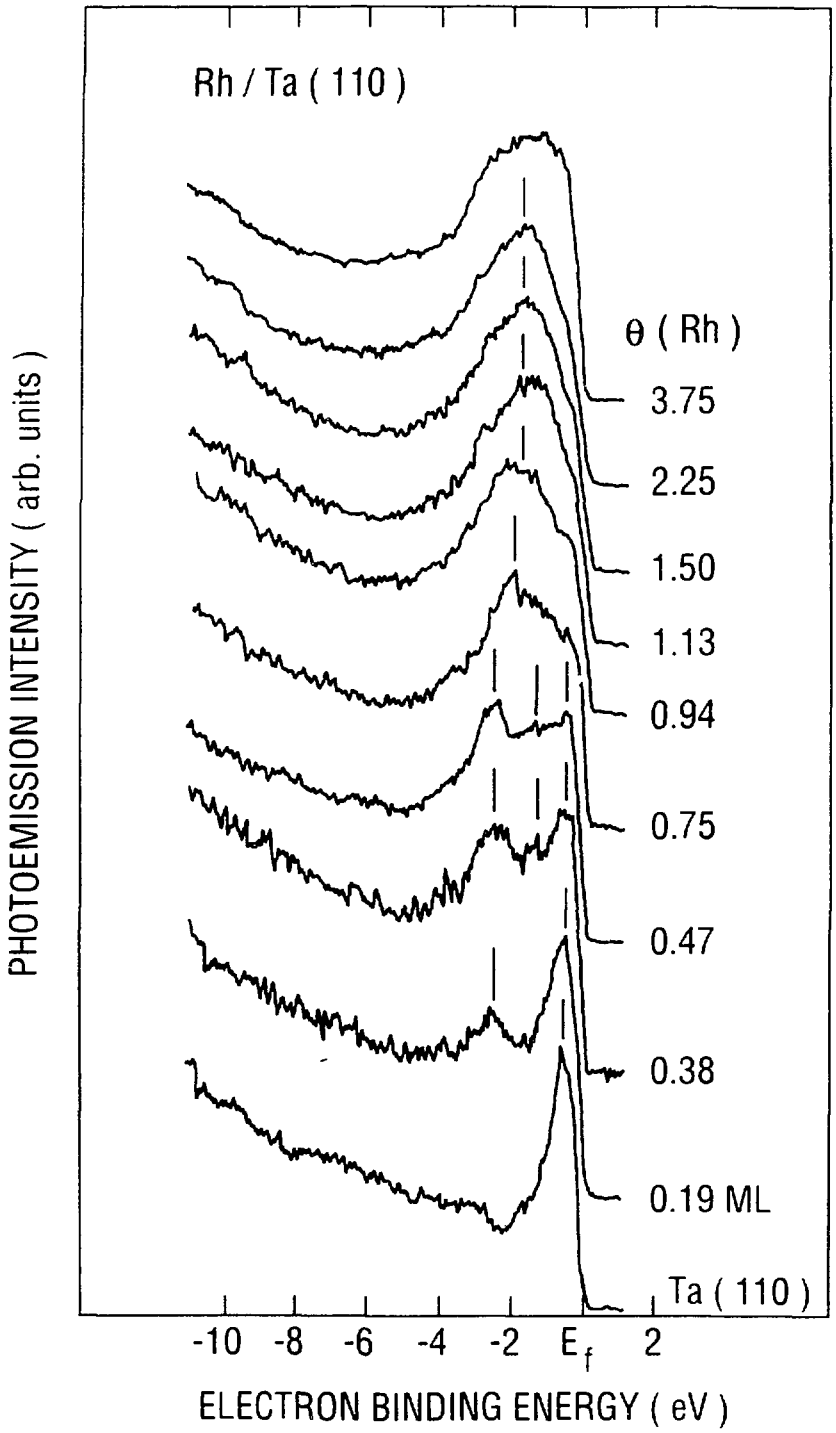
Rh / Ta (110)
θ (Rh)
3.75
2.25
1.50
1.13
0.94
0.75
0.47
0.38
0.19 ML
Ta (110)
PHOTOEMISSION INTENSITY (arb. units)
-10 -8 -6 -4 -2 E_f 2
ELECTRON BINDING ENERGY (eV)

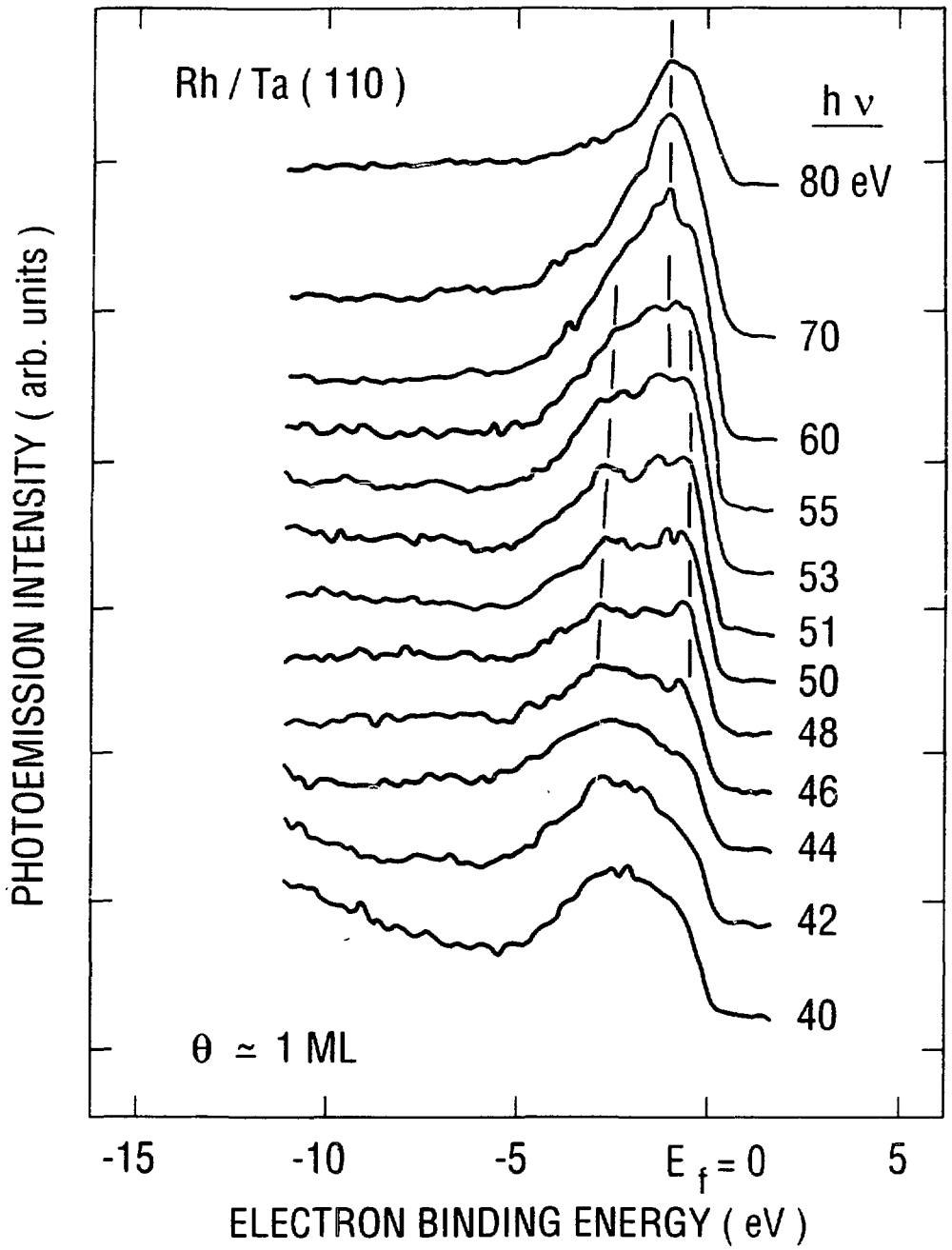
Rh / Ta (110)
h ν
80 eV
70
60
55
53
51
50
48
46
44
42
40
θ ≃ 1 ML
PHOTOEMISSION INTENSITY (arb. units)
-15
-10
-5
E f = 0
5
ELECTRON BINDING ENERGY (eV)

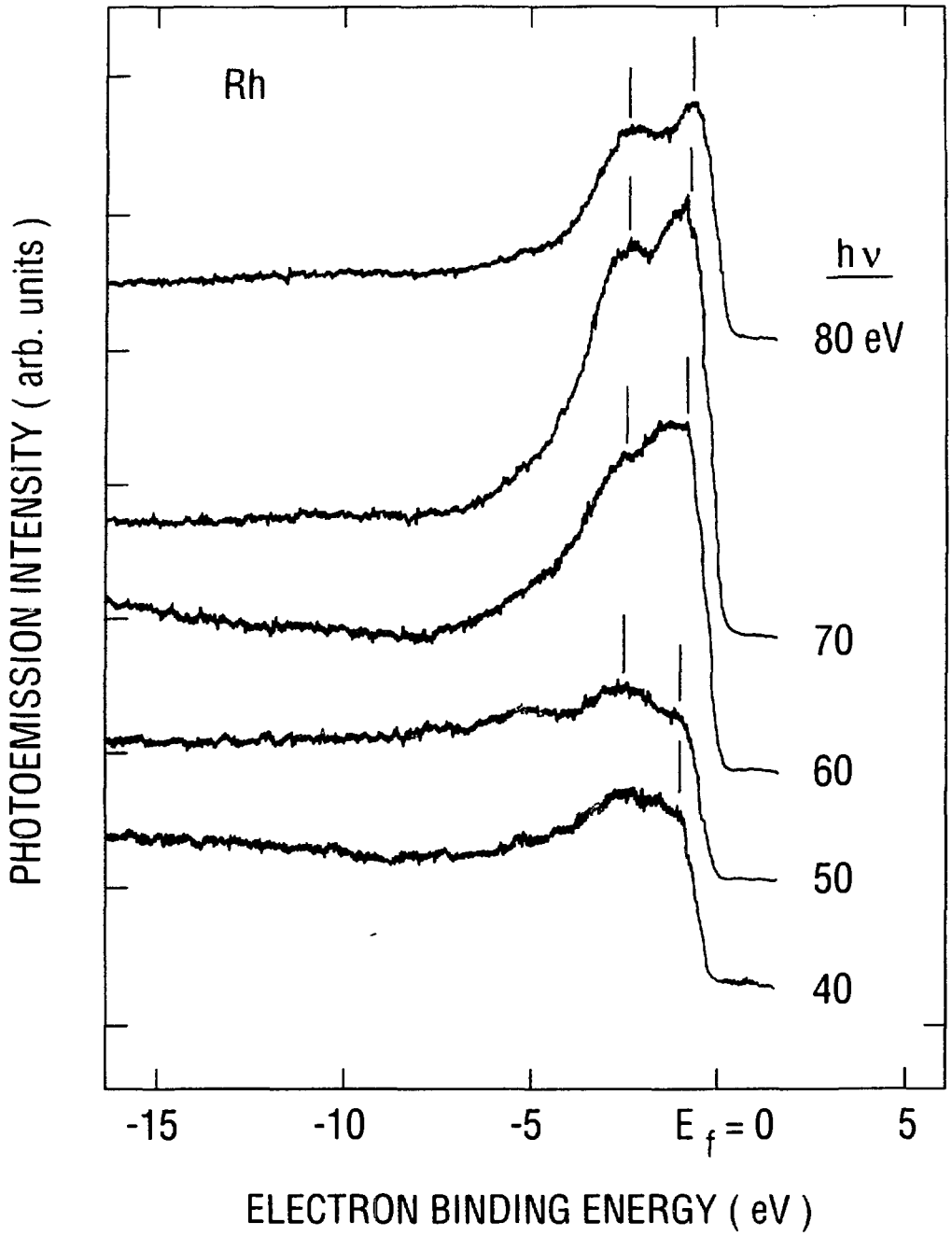
Rh
hν
80 eV
70
60
50
40
PHOTOEMISSION INTENSITY (arb. units)
-15
-10
-5
E f = 0
5
ELECTRON BINDING ENERGY (eV)

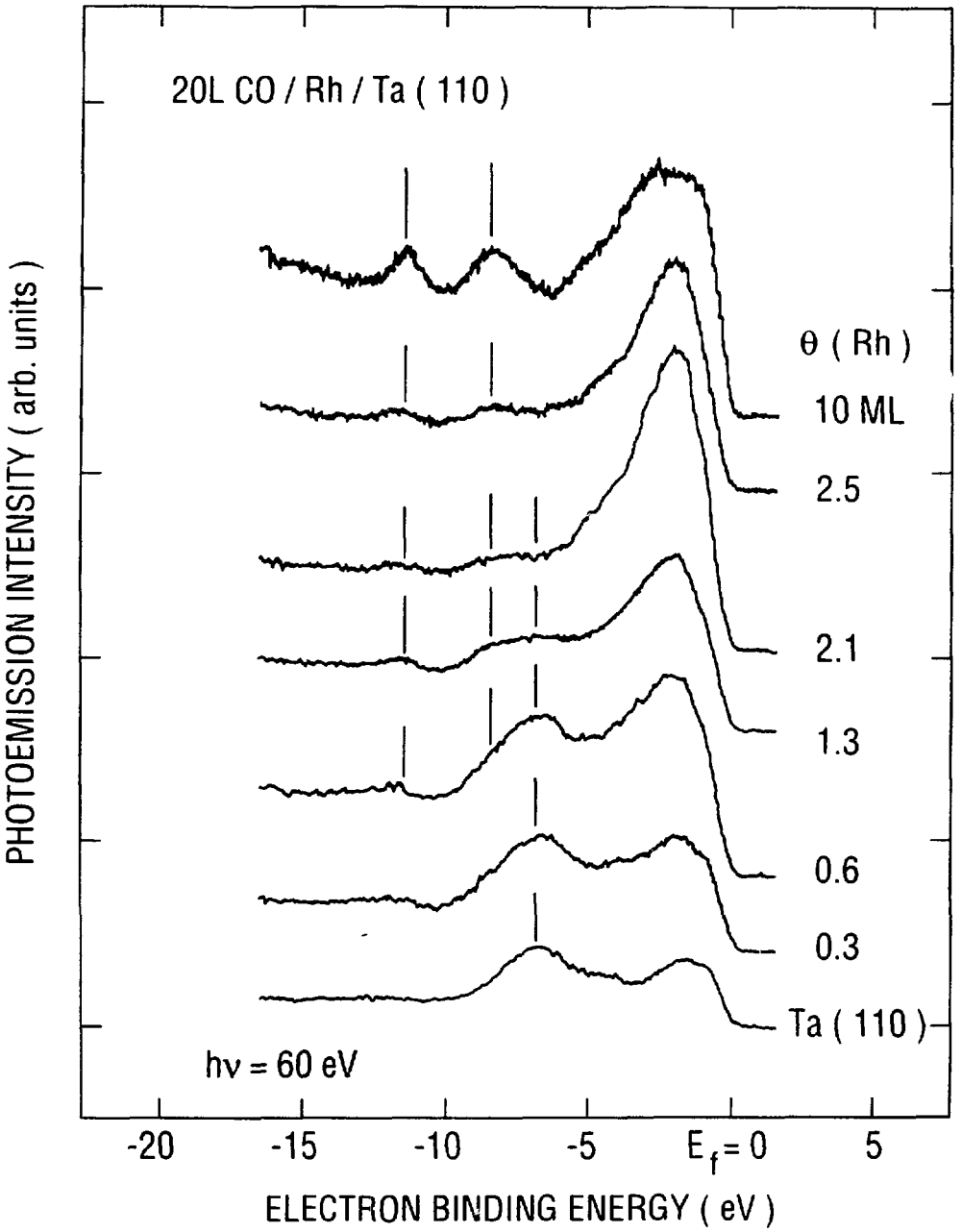
20L CO / Rh / Ta (110)
θ (Rh)
10 ML
2.5
2.1
1.3
0.6
0.3
Ta (110)
hν = 60 eV
PHOTOEMISSION INTENSITY (arb. units)
-20
-15
-10
-5
E_f = 0
5
ELECTRON BINDING ENERGY (eV)